Proceedings of ASME Turbo Expo 2022
Turbomachinery Technical Conference and Exposition
GT2022
June 13-17, 2022, Rotterdam, The Netherlands

GT2022-81982

SIMULATION OF THE HIPOWAR GAS-STEAM POWER GENERATION SYSTEM USING AMMONIA AS FUEL

Alberto Cammarata
Department of Energy
Politecnico di Milano
Milan, Italy

Paolo Colbertaldo
Department of Energy
Politecnico di Milano
Milan, Italy

Stefano Campanari
Department of Energy
Politecnico di Milano
Milan, Italy

ABSTRACT

This work presents a simulation activity on an innovative power generation cycle, developed within the EU Horizon 2020 project HiPowAR, using ammonia as fuel for an oxy-combustion process in a membrane reactor. The key advantages of the system are the low compression requirement, typical of steam cycles, and the large expander inlet temperature, typical of gas turbine cycles. The analysis explores the options of cooled or uncooled expander, either adopting a steam-cooled turbine made of conventional Ni-based alloys or using high temperature-resistant ceramic matrix composite (CMC) materials. The simulations show that, with a reactor outlet temperature of 1350°C, a cooled system could reach up to 48.2% efficiency, with limited additional advantages when further increasing the temperature. At the same temperature level, the uncooled system could instead achieve 52.5% efficiency, allowing also a substantial system simplification. However, since the expanded mixture contains nearly 90%$_{mol}$ steam, the use of CMC materials is made difficult by degradation issues and would require the development of suitable barrier coatings.

Keywords: Cycle Performance, Energy Conversion, Alternative Fuels, Power Generation, Ammonia.

NOMENCLATURE

Acronyms

BSCF	$Ba_{0.5}Sr_{0.5}Co_{0.8}Fe_{0.2}O_{3-\delta}$
CMC	Ceramic Matrix Composite
COT	Combustor Outlet Temperature
CSFM	$Ca_{0.5}Sr_{0.5}Fe_{0.2}Mn_{0.8}O_{3-\delta}$
EBC	Environmental Barrier Coating
LHV	Lower Heating Value
MR	Membrane Reactor
R	Rotor
S	Stator
RPM	Revolutions Per Minute
SCR	Selective Catalytic Reduction
TBC	Thermal Barrier Coating
TRL	Technology Readiness Level

Quantities

D	Diameter
k_{is}	Isentropic loading coefficient
u	Peripheral velocity
W	Electric power
T	Temperature
Δh_{is}	Isentropic enthalpy change
ω	Rotational speed

Subscripts

amb	Ambient
aux	Auxiliaries
el	Electric
m	Mechanical
sat	Saturation
turb	Turbine

1. INTRODUCTION

Among the alternative fuels with low carbon content, ammonia is widely investigated as a promising option for low-CO_2 emission energy processes. As a zero-carbon hydrogen-based energy vector, ammonia can be exploited in industrial processes and in power generation plants, for direct use as a fuel or extracting H_2 via a cracking process. Being liquid at relatively low pressure, ammonia offers advantages for transportability and handling, with higher volumetric energy density than gaseous or liquid hydrogen; on the other hand, it requires caution due to toxicity and it has issues of relatively low heating value and difficult ignition when used as a fuel. Ongoing research activities focus on both ammonia use in conventional processes and on the development of innovative systems for its efficient exploitation.

Regarding power generation, a significant amount of work is available in the scientific literature, which has been developed in academic and industrial R&D projects to assess the feasibility of ammonia feeding or co-firing in combustion devices or electrochemical units. Most studies suggest that ammonia must be partially cracked into hydrogen and nitrogen when used in gas

turbines or internal combustion engines due to its poor combustion characteristics. Experimental activities on spark-ignition internal combustion engines showed that it is possible to efficiently use ammonia as fuel provided that 5-15% of the input ammonia is cracked [1, 2]. The same is true for combustion in gas turbines, with a cracking requirement of 10-30% [3, 4]. Hydrocarbon-like efficiency has been demonstrated using pure NH_3 or a mixture NH_3-CH_4 in gas turbines [5]. However, the NO_x produced during the combustion process can be large due to fuel-bound nitrogen [6]. Reliable and widely usable chemical-kinetics mechanisms must be developed, in order to optimize the ammonia combustion process and minimize the NO_x emissions. Ammonia use in alkaline fuel cells also adopts a cracking unit, as proposed by GenCell [7]. Solid oxide fuel cells are able to operate on ammonia, directly or after cracking. However, the degradation mechanism induced by internal ammonia decomposition has yet to be thoroughly addressed [8].

This work investigates some advanced configurations of an innovative steam-gas power generation cycle, currently under development within the EU Horizon 2020 project HiPowAR [9]. This novel system comprises ammonia oxidation in a high-pressure membrane reactor (MR) and expansion of the resulting high-temperature steam-gas stream (H_2O+N_2) in a suitable turbine. In the MR, air is fed into thin tubular ceramic membranes that selectively allow the permeation of pure oxygen from the air side into the oxidation chamber. This occurs at high temperature (above 800°C), driven by the oxygen partial pressure gradient across the membrane. Thus, the process avoids the need for high-pressure compression of the inlet oxidant. Flameless oxy-combustion occurs at the membrane external surface, where oxygen combines with the ammonia fuel that is fed to the MR after pressurisation in liquid form with low energy requirement and regenerative evaporation. Water is injected into the reactor as a moderator, at the limited expense of liquid pumping, resulting in a large fraction of steam in the stream reaching the expander. After the oxidation process, the MR outlet stream has the high temperature typical of internal combustion cycles such as gas turbines. Overall, the HiPowAR cycle has the advantage of a limited pressurization duty thanks to the operation on the liquid phase. The system could be applied to both small- and large-scale distributed power generation as well as, in principle, to mobile applications (e.g., on ships).

This paper studies the performances of the HiPowAR power generation system under different design conditions, by means of numerical simulations, with the purpose of assessing the potential in terms of efficiency and process scheme complexity. Future work will address the experimental validation of relevant components, according to the upcoming tasks of the HiPowAR project, regarding in particular the membrane reactor, whereas this is not a critical aspect for conventional components like pumps and heat exchangers. An estimation of NO_x production rate during the oxidation process is outside the scope of this paper. However, it can be inferred that NO_x emission will be lower compared to a comparable gas turbine system due to the flameless oxidation occurring within the membrane reactor, limiting the mechanism of thermal NO_x formation. In any case, a selective catalytic reduction (SCR) reactor could be used to decrease the NO_x content in the outlet flue gas stream, using as reactant a little fraction of the ammonia already available on site.

From preliminary steady-state simulations of the HiPowAR system investigating different configurations, it was concluded that the most promising options to achieve a high efficiency involve an increase of the expander inlet temperature and an interdependent optimization of the minimum and maximum pressure. For instance, assuming an uncooled expansion, it was estimated that the efficiency could increase from 41.4% to 51.8% when increasing the turbine inlet temperature from 900°C to 1350°C [10].

Such high temperatures are challenging for the turbine blades, calling for cooling strategies. Since compressed air is not available in the system for blade cooling, an option to operate at high temperature is either the use of a different cooling fluid or the use of ceramic matrix composite (CMC) materials for the expander components, allowing for an uncooled expansion up to a target temperature as high as 1500°C [11]. However, the use of CMC materials is hampered by the high steam fraction (nearly 90%$_{mol}$), which is known to accelerate the oxidation rate of the CMC surface [12]. An alternative is to implement steam-cooled expansion adopting an open-loop coolant circuit, which allows the use of conventional Ni-based superalloys at high temperature (turbine inlet temperature up to 1500°C). The two possibilities of using CMC with a proper environmental barrier coating or cooled Ni-based alloys are investigated in this work. The additional alternative of cooling CMC blades by means of steam is instead deemed not feasible, due to material degradation issues.

Sections 2 and 3 describe the configuration of the HiPowAR system considered in this paper, the simulation methods, and the main assumptions. Section 4 shows the results in terms of turbine operating conditions, including the coolant mass flow rate required for each blade row in the cooled operation, and the system efficiency for both the cooled and the uncooled expansion configurations. For the cooled turbine case, a sensitivity analysis on the thermal barrier coating (TBC) thickness and on the coolant temperature is also included. Finally, the conclusions of the work are presented.

2. THE HIPOWAR SYSTEM

2.1 System configuration

Figure 1 shows the process scheme of the HiPowAR system. The input liquid ammonia (point #1 in Fig. 1) is pressurized (#2), evaporated (#3), and oxidized in an oxygen membrane reactor reaching a high temperature (#4). Ambient air (#15) is fed into the tubular membrane by means of a fan (not represented in Fig. 1), from which pure oxygen permeates to the high-pressure combustion zone. The O_2-depleted air (#16) is then vented into the atmosphere. Water is fed to the reactor (#14), after being pumped and preheated (#12, #13). In the MR, water acts as a moderator to limit the temperature increase driven by the oxidation reactions. To avoid having liquid droplets touching the membrane surface, water is entirely evaporated within the

reactor before entering the combustion zone, thus avoiding any risk of causing local hot spots or mechanical stress. Part of the produced steam can be collected and sent to the expander for blade cooling (#17).

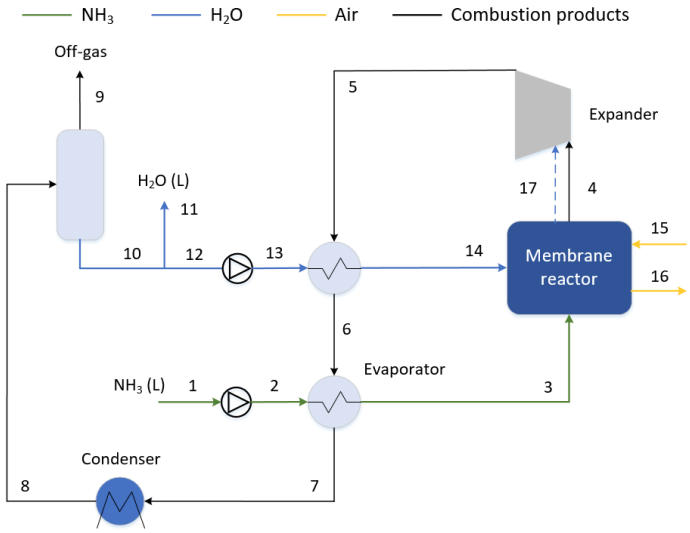

FIGURE 1: HIPOWAR SYSTEM CONFIGURATION.

The reactor outlet stream (#4) is a mixture of nearly 90%-10%$_{mol}$ H_2O-N_2 at high temperature and pressure. This is expanded to atmospheric pressure in a turbine generating useful work. After the expansion, the turbine exhaust stream (#5) is used first to preheat the cooling water, then the latent heat of stream #6 is used to entirely evaporate the input ammonia in the evaporator, maximizing the system heat integration. Complete ammonia evaporation is always possible, provided that the minimum and maximum system pressures are selected properly: at atmospheric expansion pressure, water condenses at about 100°C, while ammonia evaporates at a constant temperature of about 90°C if pressure in stream #2 is 50 bar. Therefore, a minimum temperature difference of 10°C can be kept throughout the evaporator. Note that since stream #6 is not pure water, the condensation temperature is not strictly constant, but its variation is rather low due to the large water fraction and the relatively low amount of heat exchanged while reaching the evaporator outlet (#7). Operating pressures different from the 1-50 bar combination, including sub-atmospheric expansion, were considered in [10], but here the discussion focuses on atmospheric expansion for the sake of simplicity. After the regenerative heat exchangers, heat is rejected to the environment from the condenser, and saturated nitrogen is separated and vented into the atmosphere (#9), while liquid water (#10) is recovered and partly recirculated to cool the reactor. Stream #11 represents a net water output, which is generated by the system as a byproduct.

The HiPowAR system benefits from both low compression power, typical of steam cycles, and high turbine expansion temperature, typical of gas turbine cycles. Therefore, a high efficiency is expected to be achievable by this system, which is also characterized by a relatively simple system configuration.

2.2 The membrane reactor

The membrane reactor is a crucial component of the system, which allows to develop a flameless oxy-combustion and to avoid the energy requirements for both O_2-N_2 separation and air pressurization, thanks to the adoption of oxygen-permeable ceramic membranes that allow the permeation of pure oxygen driven by the partial pressure gradient between the air stream and the oxidation chamber. Although the total pressure inside the reactor is relatively large, the oxygen partial pressure is expected to be very low since oxygen is readily consumed by the oxidation reactions; the resulting unbalance in oxygen partial pressures is the driving force for oxygen permeation.

The oxygen permeation mechanism across the membrane is shown in Fig. 2 for a generic ceramic membrane.

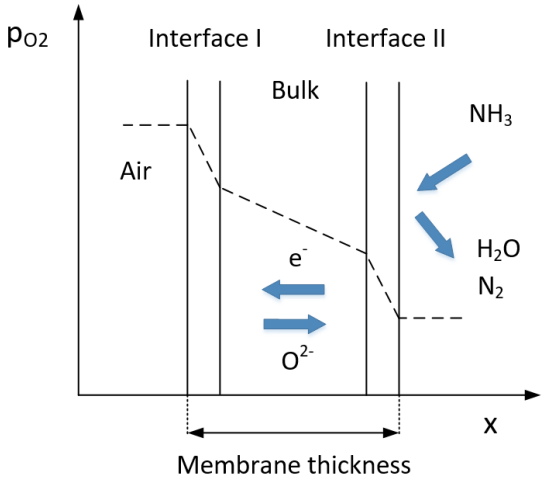

FIGURE 2: SCHEMATIZATION OF THE OXYGEN PERMEATION PROCESS DRIVEN BY ITS PARTIAL PRESSURE GRADIENT.

Molecular oxygen dissociates and recombines at interfaces I and II, respectively, whereas oxygen permeates in the form of oxygen ions (O^{2-}) through the bulk, requiring an opposite flow of electrons (e^-) to respect the electroneutrality principle. The oxygen partial pressure distribution depends on both the resistances related to bulk diffusion and the surface reactions. The interested reader may refer to the scientific literature for further details regarding ceramic oxygen membranes [13, 14].

In the HiPowAR project, a double-tube one-end-closed configuration is used for the oxygen membranes, as shown in Fig. 3. In the initial section of the tube, inlet air is heated up by recovering thermal power from the O_2-depleted air stream exiting the outer tube, without contributing to the permeation process. The remaining section ('useful length') is externally in contact with the ammonia fuel in the oxidation chamber and is responsible for oxygen permeation. The O_2-depleted air (stream #16) leaves the reactor at a relatively low temperature (e.g., 100-150°C) due to the configuration shown in Fig. 3, although the

membrane in contact with the oxidation chamber is expected to operate at high temperature (e.g., 850°C or more).

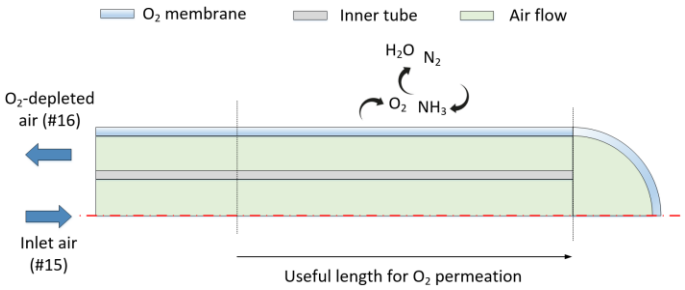

FIGURE 3: DOUBLE-TUBE ONE-END-CLOSED OXYGEN MEMBRANE CONFIGURATION.

3. METHODOLOGY

3.1 Modelling approach

The novelty of this work compared to the previous simulation efforts on the HiPowAR system [10] is to allow a wider assessment of the plant behavior, focusing on the turbine performance, by means of the integration with an advanced simulation tool able to provide a preliminary turbine design and simulate a steam-based open-loop cooled expansion. Indeed, a distinctive feature of the proposed cycle is that steam is used to cool the turbine, since compressed air is not available in the plant. Although steam is not usually employed for this purpose, some commercial gas turbines adopt steam cooling in a closed-loop configuration, mainly for cooling some parts of the combustor (combustion liners and transition ducts); in the past, a large size H-class gas turbine was also proposed by GE employing closed-loop steam cooling in the first two turbine stages [15]. In this work, only the open-loop configuration with both convective and film cooling is considered. Note that steam features better cooling properties compared to air due to a higher heat transfer coefficient [16]. However, steam cooling is not considered when CMC material blades are used, since they can be easily degraded in presence of steam [12]. Therefore, the option of cooling is coupled with the use of conventional Ni-alloys to manufacture the blades of the turbine.

The complete system is simulated using Aspen Plus®, adopting the Peng-Robinson equation of state. Among conventional components, the ammonia pump and the water pump are modelled by setting a discharge pressure of 50 bar and a total efficiency of 75%. The ammonia evaporator is modelled to guarantee complete vaporization and sized within the software via the 'design mode'. This heat exchanger operates under an approximately constant temperature difference of 10°C, for the reasons explained in Section 2.1. The heat exchanger for preheating the recirculated water is modelled by assuming a pinch-point temperature difference of 10°C. A temperature of 40°C is set at condenser outlet.

The simulation flowsheet implemented in Aspen Plus® to model the membrane reactor and the turbine, which are the most innovative elements of the process and of this work, is shown in Fig. 4. The stream numbers correspond to those in Fig. 1, the 'F' streams are fictitious streams required to represent all internal processes, the components marked with 'H' are 'Heater' components.

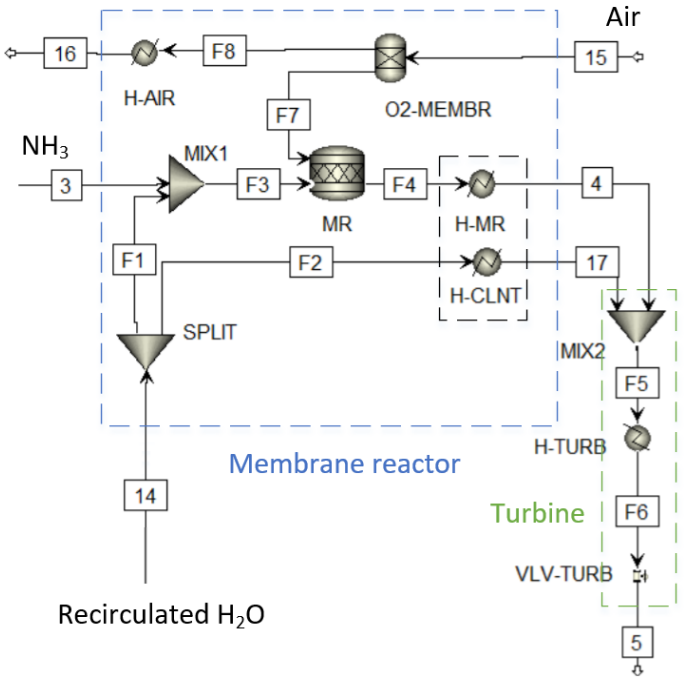

FIGURE 4: MODELLING OF MEMBRANE REACTOR AND TURBINE IN ASPEN PLUS®.

The oxygen membrane is modelled using a 'Sep' component that separates 90% of the oxygen in stream #15. The oxidation process is modelled using an 'RStoich' component ('MR'), assuming a complete oxidation process that converts the separated oxygen ('F7') via the following reaction:

$$NH_3 + 0.75\ O_2 \rightarrow 0.5\ N_2 + 1.5\ H_2O \qquad (1)$$

The oxygen flow rate that is separated and oxidized is assumed to be stoichiometric compared to the ammonia flow rate at reactor inlet (#3). Therefore, neither ammonia nor oxygen are present in stream #4. Actual kinetics may determine a different evolution of the reaction, but proper internal recirculation is expected to guarantee complete oxidation. Oxygen-depleted air is assumed to leave the reactor at 100°C after heat recovery according to the membrane configuration shown in Fig. 3. Therefore, the temperature of O_2-depleted air is increased from ambient temperature to 100°C by adding a fictitious heater component, 'H-AIR'. The duty of 'H-AIR' is added as a fictitious heat loss to the 'MR' component, together with the real heat loss assumed equal to 2% of the LHV of the inlet ammonia (#3). In the real system, the mass flow rate of steam required for expander cooling is bled from the evaporation system within the reactor at a certain temperature, here assumed equal to 350°C.

From a modelling perspective, the coolant mass flow rate predicted by the *GS* software is separated from stream #14 and sent into a fictitious heater component to reach 350°C ('H-CLNT'). The stream exiting the 'MR' component goes into the fictitious heater 'H-MR', which has a heat duty opposite to that of 'H-CLNT'. The combination of H-MR and H-CLNT represents the heat exchange in the MR to heat the coolant up to 350°C ('H-MR' and 'H-CLNT' could be replaced by a single two-side heat exchanger, but this is more likely to introduce convergence issues).

Streams #4 and #17 are then mixed together, and the resulting stream enters another heater component ('H-TURB') with a duty opposite to that of the turbine mechanical power predicted by the *GS* software, and a lamination valve with a discharge pressure equal to the atmospheric pressure.

The turbine component is modelled using the *GS* software. This software, which has been developed within the Department of Energy at Politecnico di Milano (Italy), allows to simulate complex power systems as well as single components such as a chemical reactor or an expander. Here, the *GS* software is adopted to simulate the expander behavior, allowing to estimate the generated mechanical power and the coolant mass flow rate by row of the turbine.

Hereafter, the simplified design and simulation methodology applied by *GS* for the cooled turbine, which follows the mono-dimensional approach explained in [17], is briefly outlined. The temperature, pressure, composition, and mass flow rate of the inlet turbine stream are given. Also the temperature, pressure, and composition of the coolant stream are given. The number of stages and the rotational speed are fixed (see Section 3.2). The mean diameter of the first rotor is fixed by assigning the peripheral velocity, which is varied to match the final atmospheric outlet pressure. The row mean diameter is increased linearly along the machine by a percentage of the first stator mean diameter (e.g., 3.5%). The blade height at each row inlet is found imposing a 5% overlap with respect to the previous blade exit. The stage axial chord is computed as a linear function of the mean diameter and the blade height. The reaction degree of each stage linearly increases from 0.05 to 0.4, corresponding to the first and last stage. The optimal isentropic loading coefficient for each stage is computed as a linear function of the reaction degree. The total-to-total efficiency of an uncooled stage is calculated considering penalties due to dimensional effects (if the turbine is relatively small) and operation at a suboptimal specific speed. For a cooled stage, the coolant ejected from the blade is responsible for additional fluid-dynamic losses, which are accounted for through a flow velocity reduction coefficient.

Concerning the calculation of the coolant mass flow rate required for each stage, the thermal model considers both convective and film cooling. The blade is modelled as a heat exchanger, having a constant outer stream temperature, representing the expanded gas, and an increasing temperature profile for the coolant, the blade wall, and the TBC going from the hub to the tip of the blade. For each row, the coolant mass flow rate is computed in order to have the maximum allowable blade temperature in the most critical point, which is the external surface of the blade material at the tip.

In this work, Aspen Plus® and *GS* simulations are integrated by running the two software iteratively until reaching convergence of the selected variables. The convergence variables are (i) the composition of turbine inlet stream (#4), which is an output of each Aspen Plus® run and an input for each *GS* run, (ii) the coolant mass flow rate (#17), and (iii) the turbine power output, which are outputs from each *GS* run and inputs for each Aspen Plus® run.

The system size is set by fixing the mass flow rate of stream #4 to 58.22 kg/s, as estimated in the preliminary simulations to achieve a net power output of 100 MW_m [10]. Note that if the net power output was fixed instead, the mass flow rate of stream #4 would be another convergence variable (output of the Aspen Plus® run, and input of the *GS* run), slowing down the convergence. Therefore, the efficiency values reported in the following refer to systems with a slightly variable net power output. However, size effects related to the turbine performance can be assumed negligible in the investigated cases given the large size of the system.

The main performance parameter is the electric efficiency, defined as the net electric power output of the plant divided by the thermal power of the inlet ammonia fuel computed from the LHV.

3.2 Simulation assumptions

The general assumptions used for the simulations are reported in Table 1.

TABLE 1: SIMULATION ASSUMPTIONS.

Ambient conditions	Turbine
Temperature = 25°C	Rotational speed = 7000 RPM
Pressure = 1.01325 bar	# stages = 9
	Coolant temperature = 350°C
Heat exchangers	Inlet mass flow rate = 58.22 kg/s
Minimum pinch-point = 10°C	Organic efficiency = 99.5%
Cond. outlet temperature = 40°C	Gearbox efficiency = 99.5%
Miscellaneous	Membrane Reactor
NH_3 tank pressure = $p_{sat}(T_{amb})$	MR heat loss = 2% of fuel LHV
Pressure losses are neglected	Oxygen utilization = 90%
Electric generator efficiency = 99%	Depleted air temperature = 100°C
$W_{el,aux} / W_{el,turb}$ = 1%	

Ammonia is extracted from a tank which is assumed to be in thermal equilibrium with the environment, hence the inlet liquid ammonia pressure is equal to the saturation pressure at ambient temperature. The oxygen utilization factor represents the fraction of oxygen used for ammonia oxidation in the membrane reactor, compared to the oxygen mass flow rate contained in the input air flow (stream #15 in Fig. 1). According to the assumption of complete oxidation, neither oxygen nor ammonia are present at reactor outlet; therefore, the stoichiometric oxygen amount that permeates the membrane completely oxidizes the ammonia. Pressure losses across all components are neglected for simplicity; at any rate, their impact

on the system performance is expected to be negligible due to the limited energy expenditure related to liquid pumping.

Some additional assumptions must be introduced, related to the turbine simulation, requiring as input the number of expansion stages, the rotational speed, and the coolant temperature (in case of cooled expansion). Another assumption related to the cooled configuration is the maximum allowed metal temperature. The maximum rotor temperature in a certain stage is assumed to be 30°C lower compared to the stator one, due to the larger mechanical stress acting on the blades. The maximum stator temperature is fixed at 860°C for the first stage and 830°C for the following stages. The thermal conductivity of the TBC is set to 2 W/mK [18], and its thickness is 250 μm for stators and 100 μm for rotors, corresponding to the lower bound expressed in [19].

Concerning the coolant temperature, it is assumed that steam is drawn at 350°C and 50 bar (pressure loss are not considered in this model) from the membrane reactor. Despite this temperature is higher than the saturation temperature at 50 bar (which is 264°C), which would decrease the amount of steam required for cooling, the temperature of the cooling medium cannot be too different from the temperature of the expanded gas, to avoid large thermal stresses. For the sake of simplicity, here it is assumed to keep a constant steam temperature at 350°C; however, in a next project phase, a more refined analysis would vary the steam temperature as a function of the maximum system temperature in order to minimize the amount of coolant required.

Concerning the number of stages and the rotational speed, Eq. (2) and (3) define the isentropic enthalpy drop across one stage and the peripheral speed respectively.

$$\Delta h_{is,st} = k_{is} \frac{u^2}{2} \tag{2}$$

$$u = \frac{D}{2}\,\omega \tag{3}$$

The coefficient k_{is} is limited in a certain range, hence $\Delta h_{is,st}$ can be varied by changing u through either the machine diameter or the rotational speed. At fixed ω, only the machine diameter can be used to increase the isentropic enthalpy drop across one stage. Therefore, the total isentropic enthalpy drop across the machine, which is defined by the thermodynamic conditions at inlet and outlet, can be met by either increasing the number of stages or the machine diameter. However, assuming direct coupling with the grid (3000 or 3600 RPM at 50 or 60 Hz), the total isentropic enthalpy drop featured by this application is relatively large and requires a high number of stages to limit the increase of machine diameter and keep a reasonable h/D (ratio between blade height and machine diameter) across the machine (e.g., in the center of the range 0.01-0.3). Therefore, the rotational speed is increased to limit the number of required stages. For all the simulations in this paper, it is assumed to operate the turbine at a rotational speed equal to 7000 RPM, and the number of stages is set to 9. Since the chosen rotational speed does not allow a direct coupling with the grid, a gearbox is required, with an assumed efficiency of 99.5% [20]. The assumption of a gearbox is reasonable given the low reduction ratio required to cope with the standard 50 Hz or 60 Hz grid frequency, avoiding the necessity of inverter-based power electronics.

As an additional assessment, the benefit of an increased rotational speed on the expander design is verified using AXTUR, a software for the optimal design of uncooled axial turbines developed within the Department of Energy at Politecnico di Milano (Italy) [21]. The inputs to the AXTUR code are the thermodynamic properties in the range of pressure and temperature of interest, the rotational speed, the number of expansion stages, the inlet stream temperature and pressure (1350°C and 50 bar respectively), the fluid composition (90% $_{mol}$ H_2O - 10%$_{mol}$ N_2), and the outlet pressure (1.01 bar). By using a rotational speed of 3000 RPM and 22 expansion stages, an isentropic efficiency of about 91% is estimated. Adopting a rotational speed of 7000 RPM allows achieving 93.5% isentropic efficiency while limiting the number of stages to 9. Hence, the assumption of 7000 RPM is kept.

4. RESULTS AND DISCUSSION

4.1 Cooling requirements

For the cooled configuration, Table 2 shows the mass flow rate of the required cooling steam for each blade row of the turbine. It is predicted that cooling is not required for rows after the 6th stator (out of 9 expansion stages) regardless of the MR outlet temperature, due to a sufficiently low temperature of the expanded steam-gas stream. Calculation is done assuming a maximum blade material temperature of 860°C and adopting both convective and film cooling according to the implemented cooling model [17].

TABLE 2: COOLANT MASS FLOW RATE [kg/s] REQUIRED FOR EACH BLADE ROW, AS A FUNCTION OF TEMPERATURE AT MR OUTLET.

	Temperature at MR outlet [°C]							
Row	**1100**	**1200**	**1350**	**1400**	**1450**	**1500**	**1550**	**1600**
1S	1.2	1.7	2.6	2.9	3.2	3.6	4.0	4.4
1R	0.8	1.2	1.9	2.2	2.5	2.8	3.1	3.4
2S	1.2	1.8	2.7	3.0	3.4	3.7	4.1	4.4
2R	0.8	1.3	2.2	2.6	2.9	3.2	3.6	3.9
3S	0.8	1.2	1.9	2.1	2.4	2.6	2.8	3.1
3R	0.5	0.9	1.5	1.8	2.0	2.2	2.5	2.7
4S	0.4	0.7	1.2	1.4	1.6	1.7	1.9	2.0
4R	0.0	0.4	0.9	1.1	1.3	1.4	1.6	1.8
5S	0.0	0.0	0.7	0.8	0.9	1.0	1.1	1.2
5R	0.0	0.0	0.4	0.5	0.7	0.8	0.9	1.0
6S	0.0	0.0	0.0	0.0	0.0	0.0	0.4	0.6
total	5.7	9.3	16.1	18.4	20.7	23.1	25.9	28.5

As expected, the number of cooled rows increases with the inlet temperature, since a larger pressure ratio is required to cool down the steam-gas stream below the maximum allowable metal temperature. The total required coolant mass flow rate is shown in Fig. 5 as a function of the temperature at MR outlet. Note that, despite the HiPowAR system implements a membrane reactor instead of a conventional combustor, here the temperature at reactor outlet is at any rate called 'COT' (combustor outlet temperature) for brevity and clarity.

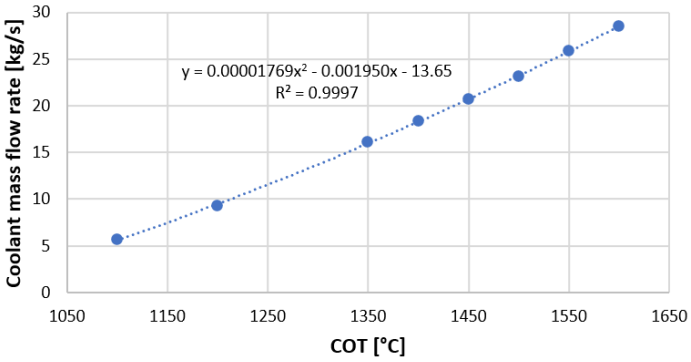

FIGURE 5: TOTAL REQUIRED COOLANT MASS FLOW RATE AS A FUNCTION OF THE TEMPERATURE AT MEMBRANE REACTOR OUTLET.

The total required coolant mass flow rate increases more than linearly with the maximum system temperature. Since the mass flow rate at the turbine inlet is fixed at 58.22 kg/s, also the ratio between the total coolant mass flow rate and that at turbine inlet increases with the turbine inlet temperature. The observed increase of this ratio with the temperature was also expected.

4.2 System performance

Figure 6 shows the system efficiency calculated at different temperatures at membrane reactor outlet, for both uncooled and cooled operation. An uncooled expansion is of course advantageous in terms of lower plant complexity, since it avoids the necessity of bleeding the coolant from the high-pressure, high-temperature membrane reactor. Moreover, an uncooled expansion is more efficient with respect to an open-loop cooled one in terms of perturbation of the expansion process.

Depending on the COT and on the material used to manufacture the blades and vanes of the turbine, stage cooling may be required or not. In Fig. 6, the point with COT equal to 850°C represents the uncooled configuration adopting a Ni-based superalloy. The remaining points of the uncooled configurations assume using CMC materials, with different COTs representing different level of technological development. All the points referring to a cooled configuration assume instead the implementation of more standard Ni-based superalloys. Steam blade cooling is not considered for CMC materials since they are subject to degradation in presence of high-temperature steam.

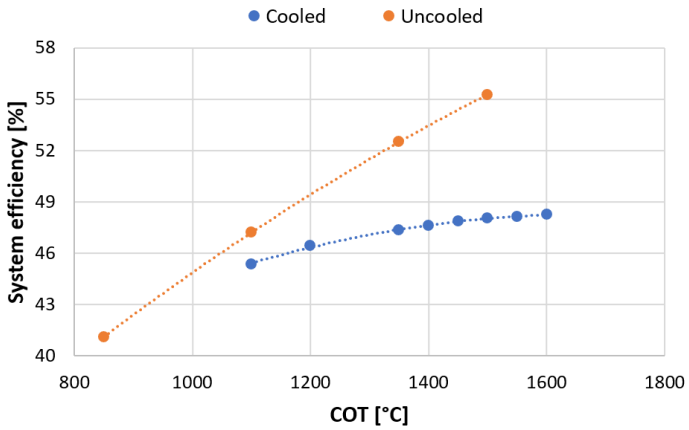

FIGURE 6: SYSTEM EFFICIENCY AS A FUNCTION OF THE TEMPERATURE AT MEMBRANE REACTOR OUTLET AND OF THE EXPANSION CONFIGURATION.

However, in this application the CMC materials are also exposed to a high steam fraction on the hot gas side (e.g., 90%$_{mol}$, much higher than in a conventional gas turbine). Therefore, additional protection layers (EBC) must be developed to protect the CMC substrate by the steam content in the expanding gas, representing an additional challenge for this application.

Despite it is possible that CMC materials could resist beyond 1350°C, another important concern is related to the oxygen membrane material. The oxygen membrane material primarily considered within the HiPowAR project is $Ba_{0.5}Sr_{0.5}Co_{0.8}Fe_{0.2}O_{3-\delta}$ (BSCF). This material shows high oxygen flux in the range 850-900°C, but it tends to creep at higher temperatures [22]. For a higher operating temperature, another membrane material has been considered, in particular $Ca_{0.5}Sr_{0.5}Fe_{0.2}Mn_{0.8}O_{3-\delta}$ (CSFM) which could withstand up to 1350°C [23]. However, it is highly difficult to further extend the operating temperature range: to the best of the authors knowledge, oxygen membrane materials capable of working beyond 1350°C are not known. Therefore, the 55.3% efficiency achieved without cooling at 1500°C is a technological challenge for the development of both suitable expander materials and oxygen membrane materials.

It should be evidenced that within the HiPowAR project, relatively low temperature levels are considered (e.g., 850°C) due to the use of BSCF as oxygen membrane material. Therefore, the development of CMC materials for the application is not a primary object for the project but could constitute a future target for a possible advancement of the technology.

From Fig. 6, the efficiency advantage of a system without blade cooling at a certain COT is clear, especially at high temperatures. At 1350°C, the HiPowAR system without blade cooling could reach 52.5% efficiency. Note that this figure is larger than a value of 51.8% found in a previous simulation effort [10], where a more conservative 90% isentropic efficiency was assumed, while the updated assessment through *GS* software allows to predict the possibility to achieve a 93.5% isentropic efficiency for this application. The performance predicted by *GS*

has been verified by using the in-house AXTUR software, as explained at the end of Section 3.

Moving to the cooled cases, if Ni-based materials are used to manufacture the turbine stages, blade cooling is required when the COT is larger than 850-900°C. In Fig. 6, only the point with COT equal to 850°C does not require cooling. The implementation of blade cooling is rather beneficial since the efficiency ranges from 41.1% at 850°C to 48.3% at 1600°C. Considering the limitations that may arise for the membrane max temperature resistance, the efficiency of 47.3%, reached at 1350°C, is also remarkable. Note that the beneficial effect of blade cooling decreases with increasing temperature, due to the increased amount of coolant, hence the potential efficiency gain above 1350°C is not so wide. For completeness, Table 3 reports the thermodynamic conditions calculated for each of the streams in Fig. 1, for the cooled configuration with a COT equal to 1350°C.

TABLE 3: THERMODYNAMIC CONDITIONS CALCULATED FOR ALL STREAMS ASSUMING A COOLED CONFIGURATION WITH A COT EQUAL TO 1350°C (MOLAR COMPOSITIONS ARE REPORTED).

#	T [°C]	p [bar]	m [kg/s]	NH_3	H_2O	N_2	O_2	H_2O (L)
1	25	10	12.5	100	0	0	0	0
2	26	50	12.5	100	0	0	0	0
3	89	50	12.5	100	0	0	0	0
4	1350	50	58.2	0	87.8	12.2	0	0
5	419	1	74.3	0	90.6	9.4	0	0
6	99	1	74.3	0	84.7	9.4	0	5.9
7	99	1	74.3	0	75.6	9.4	0	15.0
8	40	1	74.3	0	0.6	9.4	0	90.0
9	40	1	10.8	0	6.2	93.8	0	0
10	40	1	63.5	0	0	0	0	100
11	40	1	19.4	0	0	0	0	100
12	40	1	44.1	0	0	0	0	100
13	40	50	44.1	0	0	0	0	100
14	263	50	44.1	0	7.2	0	0	92.8
15	25	1	84.3	0	0	79.0	21.0	0
16	100	1	66.6	0	0	97.4	2.6	0
17	350	50	16.1	0	100	0	0	0

Regarding the system cost, at the current development stage it is challenging to make an accurate assessment, due to the peculiarity of some of the components, in particular the membranes and the gas-steam expander, which are not commercial products. The membrane reactor is expected to represent a significant share of the system investment cost (e.g., 50%, from preliminary project estimates) due to both membrane manufacturing and reactor assembly. Moreover, the turbine envisaged for this application is a non-commercial component due to the peculiar pressure-temperature-composition combination at expander inlet. The expanded fluid is mainly steam, but the high temperature required for this application does not allow the use of conventional steam expanders, which can typically withstand a maximum temperature of about 600°C. At any rate, it is expected that the final cost of the system will improve along the evolution of the TRL from the prototype or pilot-scale system (current TRL 3 to 4) to a full-scale mature and commercial stage. After the experimental validation of the technologies, improvements in engineering and manufacturing will be crucial for the success of the HiPowAR process.

4.3 Sensitivity analysis

This section presents the results of a sensitivity analysis on both the TBC thickness and the coolant temperature, in order to evaluate their impact on the performance of the cooled-expander configuration. The results presented in Section 4.2 assumed a TBC thickness of 250 μm for stators and 100 μm for rotors, corresponding to the lower bound expressed in [19]. Increasing the TBC thickness of stators and rotors to their upper bound values, equal to 500 μm and 250 μm, respectively, allows reaching a system efficiency of 48.1% at a COT of 1350°C, which is 1.6% larger than that computed with lower TBC thickness. Although the efficiency increase is not negligible, the uncooled system still performs significantly better, offering a system efficiency of 52.5% at the same temperature level. Hence, it is concluded that a change in the TBC thickness is not relevant for the main results of the analysis. Nevertheless, adopting a thicker TBC reduces the overall required coolant mass flow rate from 16.1 to 13.1 kg/s, as shown in Table 4, which may be beneficial from the manufacturing point of view.

TABLE 4: SENSITIVITY ANALYSIS ON TBC THICKNESS (t_{TBC} IS INCREASED BY 100% AND 150% FOR STATORS AND ROTORS, RESPECTIVELY, COMPARED TO BASELINE) AND COOLANT TEMPERATURE (300 vs. 350°C) AT COT=1350°C.

	Baseline	Thicker TBC	Thicker TBC & lower $T_{coolant}$
System efficiency [%]	47.3	48.1	48.2
Coolant mass flow rate [kg/s]	16.1	13.1	12.0
# cooled rows	10	10	10

Finally, a simulation with a coolant temperature of 300°C is performed. This corresponds to about 36°C of superheating compared to the saturated condition at 50 bar. It is expected that the system efficiency would increase due to the lower coolant mass flow rate required for the same cooling effect. However, adding also this modification yields only a marginal efficiency gain (the efficiency is 48.2% vs. 48.1%) compared to the case with a coolant temperature of 350°C at equally increased TBC thickness. It can be concluded that the assumption regarding the coolant temperature is not of primary importance for the results presented, whereas it could be of interest for the coolant mass flow rates. Since both the mass flow rate and the coolant temperature are lower compared to the baseline case, the number

of cooled rows could increase due to a larger temperature of the expanded fluid. However, this is not the case for the considered condition of COT=1350°C.

5. CONCLUSION

This paper has presented a simulation activity regarding the HiPowAR power generation system, which implements an oxygen membrane reactor that avoids the large energy consumption required for oxidant compression in conventional gas turbines cycles. The main focus of this work is the simulation of a cooled expansion, which allows considering the use of Ni-based alloys to manufacture the turbine stages that must operate in a high-temperature environment. This is then compared to the option of uncooled operation at high temperature (e.g., 1350°C), using CMC materials.

For the cooled system, it is concluded that it is not advantageous to push the reactor outlet temperature above 1350°C, both for the limited efficiency increase and for the unavailability of oxygen membranes working in that temperature range. The analysis shows that uncooled operation has a large efficiency advantage compared to a configuration implementing a cooling system, especially when the COT is large. In particular, considering a temperature of 1350°C, the uncooled system based on CMC materials achieves 52.5% efficiency, which is quite attractive compared to the 48.2% efficiency obtained with Ni-based alloys and the implementation of a cooling system. Moreover, the absence of a cooling system allows for a simpler system design. However, cooling allows to avoid the use of CMC materials, which are costly and can be degraded by the presence of steam (which is about 90%$_{mol}$ in this application), requiring the development of a suitable environmental barrier coating (EBC) to withstand the expander operating conditions.

ACKNOWLEDGEMENTS

The HiPowAR project has received funding from the European Union's Horizon 2020 research and innovation programme under grant agreement n. 951880.

REFERENCES

[1] Mørch, C. S., Bjerre, A., Gøttrup, M. P., Sorenson, S. C., Schramm, J., 2011, "Ammonia/hydrogen mixtures in an SI-engine: engine performance and analysis of a proposed fuel system" Fuel, 90, pp. 854–864.

[2] Lhuillier, C., Brequigny, P., Contino, F., Mounaïm-Rousselle, C., 2019, "Performance and Emissions of an Ammonia-Fueled SI Engine with Hydrogen Enrichment", SAE Technical Paper 2019-24-0137, 14th International Conference on Engines & Vehicles.

[3] Khateeb, A. A., Guiberti, T. F., Zhu, X., Younes, M., Jamal, A., Roberts, W. L., 2020, "Stability limits and NO emissions of technically-premixed ammonia-hydrogen-nitrogen-air swirl flames", International J. of Hydrogen Energy, 45, pp. 22008–22018.

[4] Verkamp, F. J., Hardin, M. C., Williams, J. R., 1967, "Ammonia combustion properties and performance in gas-turbine burners", Symposium (International) on Combustion, 11, pp. 985–992.

[5] Kurata, O., Iki, N., Matsunuma, T., Inoue, T., Tsujimura, T., Furutani, H., Kobayashi, H., Hayakawa, A., 2016, "Performances and emission characteristics of NH_3-air and NH_3-CH_4-air combustion gas-turbine power generations", Proc. Combust. Inst., 36, pp. 3351–3359.

[6] Kurata, O., Iki, N., Matsunuma, T., Inoue, T., 2017, "Success of ammonia-fired, regenerator-heated, diffusion combustion gas turbine power generation and prospect of low NOx combustion with high combustion efficiency", Proc. of ASME Power Conf. Joint with ICOPE-17, POWER-ICOPE2017-3277.

[7] Gencell A5 – off-grid power solution. https://www.gencellenergy.com/our-products/gencell-a5/ (accessed December 22, 2021)

[8] Kishimoto, M., Muroyama, H., Suzuki, S., Saito, M., Koide, T., Takahashi, Y., Horiuchi, T., Yamasaki, H., Matsumoto, S., Kubo, H., Takahashi, N., Okabe, A., Ueguchi, S., Jun, M., Tateno, A., Matsuo, T., Matsui, T., Iwai, H., Yoshida, H., Eguchi, K., 2020, "Development of 1 kW-class ammonia-fueled solid oxide fuel cell stack", Fuel Cells, 20, pp. 80–88.

[9] HiPowAR project website. https://www.hipowar.eu/en/home (accessed December 21, 2021).

[10] Cammarata, A., Colbertaldo, P., Campanari, S., 2021, "Simulation of the HiPowAR power generation system for steam-nitrogen expansion after ammonia oxidation in a high-pressure oxygen membrane reactor", E3S Web Conf., 312, Proc. of 76th Italian National Congress ATI, 08016.

[11] Hurst, J., 2018, "Nasa transformational tools technologies project: 2700°F CMC/EBC technology challenge", Proc. of ASME Turbo Expo, GT2018-77282.

[12] Tejero-Martin, D., Bennett, C., Hussain, 2021, T., "A review on environmental barrier coatings: hystory, current state of the art, and future developments", J. of the European Ceramic Society, 41, pp. 1747–1768.

[13] Sunarso, J., Baumann, S., Serra, J. M., Meulenberg, W. A., Liu, S., Lin, Y. S., Diniz da Costa, J. C., 2008, "Mixed ionic-electronic conducting (MIEC) ceramic-based membranes for oxygen separation", J. of Membrane Science, 320, pp. 13–41.

[14] Zhu, X., Liu, H., Cong, Y., Yang, W., 2011, "Permeation model and experimental investigation of mixed conducting membranes", AIChE Journal, 58, pp. 1744–1754.

[15] Smith, R. W., Polukort, P., Maslak, C. E., Jones, C. M., Gardiner, B. D., 2001, "Advanced Technology Combined Cycles", GE Power Systems report GER-3936A.

[16] Xu, L., Wang, W., Gao, T., Shi, X., Gao, J., Liang, W., 2014, "Experimental study on cooling performance of a steam-cooled turbine blade with five internal cooling smooth channels", Experimental Thermal and Fluid Science, 58, pp. 180–187.

[17] Chiesa, P., Macchi, E., 2004, "A thermodynamic analysis of different options to break 60% electric efficiency in combined cycle power plants", J. Eng. Gas Turbines Power, 126, pp. 770–785.

[18] Wee, S., Do, J., Kim, K., Lee, C., Seok, C., Choi, B., Choi, Y., Kim, W., 2020, "Review on mechanical thermal properties of superalloys and thermal barrier coating used in gas turbines", Appl. Sci., 10, 5476.

[19] Darolia, R., 2013, "Thermal barrier coatings technology: critical review, progress update, remaining challenges and prospects", International Material Reviews, 58:6, pp. 315–348.

[20] Lozza, G., 1990, "Bottoming steam cycles for combined gas-steam power plants: a theoretical estimation of steam turbines performances and cycle analysis", ASME COGEN-TURBO Symposium, pp. 83–92.

[21] Macchi, E., Astolfi, M., 2017, *Organic rankine cycle (ORC) power systems*, Woodhead Publishing.

[22] Rutkowski, B., Malzbender, J., Beck, T., Steinbrech, R. W., Singheiser, L., 2011, "Creep behaviour of tubular $Ba_{0.5}Sr_{0.5}Co_{0.8}Fe_{0.2}O_{3-\delta}$ gas permeation membranes", J. of the European Ceramic Society, pp. 493–499.

[23] Kriegel, R., Jager, B., Kircheisen, R., 2019, "Production of N_2-free syngas by methane combustion with consecutive reforming", Key Note Lecture, 14th ICCMR.